Electronic Supplementary Information for

Ladder-Like Polyacetylene with Excellent Optoelectronic Properties and Regular Architecture

Wei Song, Huijing Han, Jianhua Wu, and Meiran Xie*

Department of Chemistry, East China Normal University, Shanghai 200241, China

*Corresponding author. Tel.: +86 21 54340058; Fax: +86 21 54340058

E-mail address: mrxie@chem.ecnu.edu.cn

Experimental

Characterization

^{1}H (500 MHz) and ^{13}C (125 MHz) NMR spectra were recorded using tetramethylsilane as an internal standard on a Bruker DPX spectrometer. Melting Point was determined by X-4B apparatus. The HR-ESIMS was measured by a Bruker QTOF micromass spectrometer. IR spectra were recorded by Perkin Elmer Spectrum One FTIR spectrophotometer. UV-vis absorption spectra were measured on a UV-1800 spectrometer. Gel permeation chromatography (GPC) was used to calculate relative molecular weight and molecular weight distribution equipped with a Waters 1515 Isocratic HPLC pump, a Waters 2414 refractive index detector, and a set of Waters Styragel columns (7.8 × 300 mm, 5 mm bead size; 10^3, 10^4, and 10^5 Å pore size). GPC measurements were carried out using THF or 1,2,3-trichlorobenzene as the eluent with a flow rate of 1.0 mL/min. The system was calibrated with polystyrene standard. Thermal gravimetric analysis (TGA) was performed using an SDTA851e/SF/1100 TGA instrument under nitrogen flow at a heating rate of 10 ^{o}C/min from 50 to 800 ^{o}C. Samples for transmission electron microscopy (TEM) were prepared by depositing a drop of the solution (1 mg/mL) on a carbon coated Cu grid, and TEM images were recorded on the JEOL2100F microscopes operating at 120 kV. Cyclic voltammetry was carried out with an Autolab PGSTAT12 potentiostat from Eco Chemie coupled to an electrochemical cell with three electrodes. The scan rate is 100 mV s^{-1}. A glassy carbon electrode was used as working electrode, a Pt wire as counter, and Ag/AgCl was used as the reference electrode. 0.1 M Bu_4NPF_6 of CH_3CN solution was used as the supporting electrolyte, and Fc^{+}/Fc was used as the reference.

Materials

4-Hydroxymethyl-1,6-heptadiyne, 2-(2-propinyl)-4-pentinoic acid, and didodecyl dipropargylmalonate (DDDPM) were prepared by the same method from the previous literature.[1] Solvents were distilled over drying agents under nitrogen prior to use: dichloromethane (CH_2Cl_2), chloroform ($CHCl_3$) and dimethylformamide (DMF) from calcium hydride. The third generation Grubbs catalyst was prepared according to the synthetic procedure in literature.[2] 1,6,7,12-Tetrachloroperylene-3,4:9,10-tetracarboxylic dianhydride was purchased from commercial sources at analytical grade and used without further purification. 12-Amino dodecanoic acid was obtained from Alfa Aesar. Glacial acid (HAc) and propionic acid were purchased

from Shanghai Chemical Reagents Co., and used as received without purification. 1-(3-Dimethylaminopropyl)-3-ethylcarbodiimide hydrochloride (EDCI·HCl), 4-dimethylaminopyridine (DMAP), 2-aminoethanol, and 2-ethylhexylamine were purchased from Energy Chemical. All reactions were carried out under dry nitrogen atmospheres using standard Schlenk-line techniques.

Experimental procedure for monomer syntheses (1 - 3)

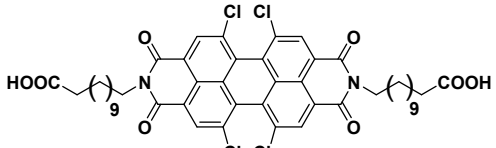

1a

A mixture of 1,6,7,12-tetrachloroperylene-3,4:9,10-tetracarboxylic dianhydride (2.65 g, 5 mmol) and 12-amino dodecanoic acid (2.58 g, 12 mmol) in propionic acid (40 mL) was heated to reflux at 140 ^{o}C for 36 h under a N_2 atmosphere. The resulting mixture was cooled and poured into water, filtrated, and washed with water until the filtrate reached neutrality. The crude solid was dried 70 ^{o}C under vacuum. After being purified by column chromatography on silica gel using a mixture of HAc/CH_2Cl_2 1/150 to 1/125 as eluent, the product **1a** was obtained as an orange-red powder (4.02 g, 4.3 mmol, 87 %); ^{1}H NMR (500 MHz, $CDCl_3$, ppm): δ 8.69 (s, 4H, pery), 4.32-4.18 (m, 4H, NC*H*$_2$CH$_2$), 2.45-2.31 (m, 4H, CH$_2$C*H*$_2$COOH), 1.82-1.71 (m, 4H, NCH$_2$C*H*$_2$), 1.70-1.62 (m, 4H, C*H*$_2$CH$_2$COOH), 1.55-1.18 (m, 28H, CH$_2$C*H*$_2$CH$_2$); ^{13}C NMR (125 MHz, $CDCl_3$, ppm): δ 178.78, 161.94, 134.75, 132.61, 130.81, 128.67, 123.29, 40.43, 33.42, 29.04, 28.68, 27.58, 26.48, 24.10.

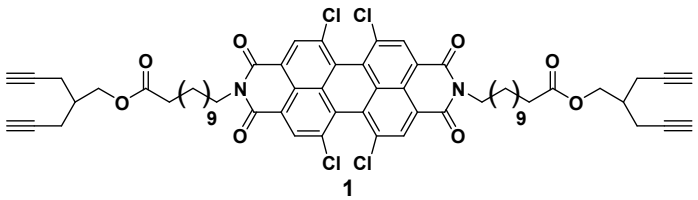

1

Compound **1a** (2.50 g, 2.7 mmol) was firstly dissolved in 10 mL of anhydrous DMF and 70 mL of $CHCl_3$. To this solution, 2-(2-propinyl)-4-pentinoic acid (1.32 g, 10.8 mmol), EDCI·HCl (1.24 g, 6.5 mmol) and DMAP (0.1 g, 0.8 mmol) were added under a N_2 atmosphere in ice-water bath for 2 h, then the reaction progress proceeded at room temperature and was monitored by TLC. After 3 days, the mixture was evaporated to remove CH_2Cl_2 and then poured to 400 mL of water to precipitate dark red solid. The solid was purified by column chromatography on silica gel using

CH_2Cl_2 as eluent. The product **1** was obtained as a red powder (2.01 g, 66 %); ^{1}H NMR (500 MHz, $CDCl_3$, ppm): δ 8.69 (s, 4H, pery), 4.26-4.18 (t, 4H, NCH_2CH$_2$), 4.17-4.12 (d, 4H, *J* = 6.10 Hz, OCH_2CH), 2.45-2.36 (dd, 4H, *J* = 2.64, 6.40 Hz, CH_2COOCH$_2$), 2.34-2.27 (t, 8H, *J* = 7.48 Hz, CHCH_2CCH), 2.22-2.09 (m, 2H, CH$_2$C*H*CH$_2$), 2.02 (t, 4H, *J* = 2.55 Hz, CH$_2$CC*H*), 1.82-1.69 (m, 4H, NCH$_2$CH_2), 1.68-1.52 (m, 4H, CH_2CH$_2$COOH), 1.51-1.19 (m, 28H, CH_2); ^{13}C NMR (125 MHz, $CDCl_3$, ppm): δ 174.13, 162.11, 135.70, 131.83, 129.11, 123.28, 80.98, 70.51, 65.08, 41.03, 36.36, 34.44, 29.59, 28.08, 27.06，25.00, 19.86; ESI-MS: Calcd. For $C_{64}H_{66}Cl_4N_2O_8Na$ $[M+Na]^+$: 1153.3508, Found: 1153.3465.

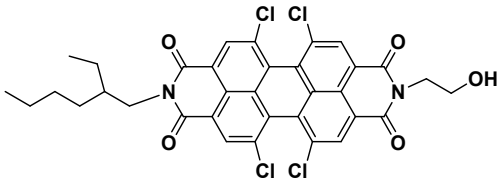

2a

Compound **2a** was synthesized by literature procedure.[3] To a suspension of 1,6,7,12-tetrachloroperylene-3,4:9,10-tetracarboxylic dianhydride (2.65 g, 5 mmol) in 30 mL of toluene, 2-ethylhexylamine (0.69 g, 5.4 mmol) and ethanolamine (0.33 g, 5.4 mmol) were added and stirred under a N_2 atmosphere at reflux for 24 h. After being cooled to room temperature, 100 mL of CH_2Cl_2 was added, obtaining a red precipitate. The CH_2Cl_2 phase was evaporated to remove solvent, and purified by column chromatography on silica gel using CH_2Cl_2/EA (10:1) as eluent. The product **2a** was obtained as a dark red powder (1.08 g, 25 %); ^{1}H NMR (500 MHz, $CDCl_3$, ppm): δ 8.68 (s, 4H, pery), 4.56-4.39 (t, 2H, *J* = 5.08 Hz, NCH_2CH$_2$OH), 4.19-4.06 (t, 2H, *J* = 5.98 Hz, NCH$_2$CH_2OH), 4.04-3.93 (d, 2H, *J* = 5.13 Hz, NCH_2CH), 1.95 (s, 1H, NCH$_2$CH$_2$O*H*), 1.89-1.69 (m, 1H, NCH$_2$C*H*CH$_2$), 1.43-1.13 (m, 8H, CH_2 on ethylhexyl), 1.01-0.80 (m, 6H, CH_3).

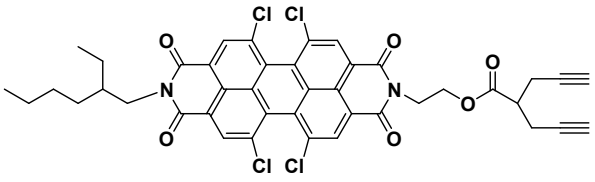

2

To a solution of **2a** (2.34 g, 3.4 mmol) in 50 mL anhydrous CH_2Cl_2, 2-(2-propinyl)-4-pentinoic acid (0.93 g, 6.8 mmol), EDCI·HCl (2.20 g, 12 mmol) and

DMAP (0.2 g, 1.6 mmol) were added under stirring at ice-water bath for 2 h, then the reaction progress proceeded at room temperature and was monitored by TLC. After 2 days, the mixture was washed with water, dried with $MgSO_4$, and evaporated to remove CH_2Cl_2. The solid was purified by column chromatography on silica gel using CH_2Cl_2/petroleum (1:1) as eluent. The product **2** was obtained as an red powder (2.46 g, 3 mmol, 90 %); ^{1}H NMR (500 MHz, $CDCl_3$, ppm): δ 8.65 (s, 4H, pery), 4.5-4.48 (t, 8H, OC*H*$_2$CH$_2$N+OCH$_2$C*H*$_2$N), 4.21-4.08 (d, 2H, NC*H*$_2$CH), 2.77-2.68 (m, 1H, CH$_2$C*H*COO), 2.67-2.52 (d, 4H, CHCC*H*$_2$), 1.98-1.89 (m, 1H, CH$_2$C*H*CH$_2$), 1.86 (s, 2H, C*H*CCH$_2$), 1.48-1.26 (m, 8H, C*H*$_2$ on ethylhexyl), 1.00-0.82 (m, 6H, C*H*$_3$); ^{13}C NMR (125 MHz, $CDCl_3$, ppm): δ 174.25, 161.41, 134.48, 132. 30, 130.46, 127.20, 122.81, 121.35, 79.48, 69.28, 61.26, 43.79, 41.24, 38.57, 37.03, 29.64, 27.69, 23.01, 22.04, 18.88, 13.11, 9.63; ESI-MS: Calcd. For $C_{42}H_{32}Cl_4N_2O_6Na$ $[M+Na]^+$: 823.0860, Found: 823.0907.

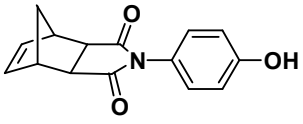

exo-**NDI**

To a suspension of 4-aminophenol (3.27 g, 30 mmol) in HAc (60 mL), bicyclo[2.2.1]hept-5-ene-2,3-dicarboxylic anhydride (4.97 g, 30 mmol) was added. After stirring at 80 °C for 1 hour, the mixture gradually became clear. One day later, the mixture was cooled and the product precipitated. Recrystallization from ethanol for 2 times to give 6.82 g needle crystalline solid in 89 % yield, m.p.: 271-273 °C; ^{1}H NMR (500 MHz, CD_3OD, ppm): δ 7.06-6.99 (d, 2H, *J* = 8.70 Hz, NCC*H*), 6.87-6.80 (d, 2H, *J* = 9.02 Hz, OCCH), 6.37 (s, 2H, C*H*=CH), 3.28-3.23 (s, 2H, CHC*H*CO), 2.83 (s, 2H, CH=CHC*H*), 1.63-1.42 (m, 2H, CHC*H*$_2$CH); ^{13}C NMR (125 MHz, CD_3OD, ppm): δ178.36, 157.14, 137.30, 127.40, 123.19, 115.45, 45.29, 42.01; ESI-MS: Calcd. For $C_{17}H_{15}NO_4$ Na $[M+Na]^+$: 278.0792, Found: 278.0788.

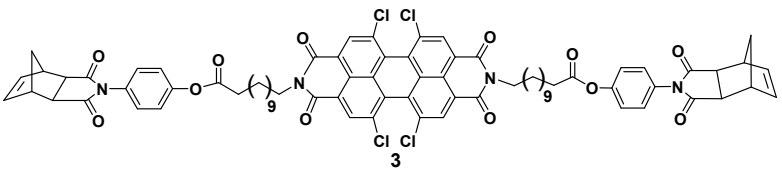

3

To a solution of **1a** (1.59 g, 1.7 mmol) in 30 mL of anhydrous 1,4-dioxane and 30 mL of CH_2Cl_2, *exo*-**NDI** (1.05 g, 4.1 mmol), EDCI·HCl (0.97 g, 5.1 mmol), and DMAP (0.08 g, 0.7 mmol) were added under stirring at ice-water bath for 2 h, then

the reaction progress proceeded at room temperature for 3 days. The mixture was evaporated to remove solvent. The solid was purified by column chromatography on silica gel using CH_2Cl_2/$(CH_3)_2CO$ (150:1) as eluent. 2.02 g red powder **3** was obtained in 85 % yield; ^{1}H NMR (500 MHz, $CDCl_3$, ppm): δ 8.69 (s, 4H, pery), 7.35-7.29 (dd, 4H, *J* = 2.15, 6.82 Hz, NCC*H*), 7.24-7.17 (dd, 4H, *J* = 2.17, 6.82 Hz, OCC*H*), 6.36 (s, 4H, C*H*=CH), 4.27-4.18 (t, 4H, *J* = 7.54 Hz, NCH_2CH_2), 3.42 (s, 4H, COC*H*CH), 2.86 (s, 4H, C*H*CH=CH), 2.61-2.54 (t, 4H, *J* = 7.55 Hz, CH_2COO), 1.84-1.24 (m, 40H, $CH_2CH_2CH_2$+CHCH_2CH); ^{13}C NMR (125 MHz, $CDCl_3$, ppm): δ 176.86, 171.80, 162.25, 150.49, 139.01, 135.36, 132.93, 131.44, 129.12, 128.59, 127.29, 123.27, 122.29, 67.10, 47.83, 45.96, 42.99, 40.97, 34.39, 29.10, 27.05, 24.99; ESI-MS: Calcd. For $C_{62}H_{40}Cl_4N_4O_{12}Na$ $[M+Na]^+$: 1399.8187, Found: 1399.8192.

General procedure for polymerization

Typically, polymerization was carried out in a Schlenk tube under dry nitrogen atmosphere at 50 °C in $CHCl_3$ or THF for a preset time. After confirmed the monomer conversion by TLC, a small amount of ethyl vinyl ether was added to the mixture and stirring for 1 h, the reaction mixture was concentrated and poured into an excess of acetone. The dark red polymer was washed successively with acetone, and dried in a vacuum oven at 40 °C to a constant weight.

A 250 mL Schlenk tube was charged with monomer **1** (50 mg, 0.04 mmol) dissolved in 67 mL of $CHCl_3$. In another 10 mL Schlenk tube, **Ru-III** (1.4 mg, 1.6 μmol) was dissolved in $CHCl_3$ (0.5 mL). After degassed with three freeze-vacuum-thaw cycles, the catalyst solution of **Ru-III** was then injected into the monomer solution via a syringe under vigorous stirring at 50 °C for 1 h. ^{1}H NMR (500 MHz, $CDCl_3$, ppm): δ 8.55 (s, Pery), 6.53 (s, C*H*=C*H* on backbone), 4.35-3.70 (m, OCH_2+CH_2N), 3.06-1.98 (m, CH_2COO+CH_2C*H*CH_2), 1.83-0.92 (m, NCH_2(CH_2)$_9$CH_2COO); ^{13}C NMR (125 MHz, $CDCl_3$, ppm): δ 172.86, 161.29, 137.63, 135.02, 134.33, 132.10, 130.49, 127.52, 122.25, 66.74, 39.60, 35.27, 33.64, 27.67, 26.68, 25.35, 24.02.

Monomer **2** (50 mg, 0.06 mmol) and **Ru-III** (2.1 mg, 2.4 μmol) were stirred in 0.5 mL of $CHCl_3$ at 50 °C for 1 h. ^{1}H NMR (500 MHz, $CDCl_3$, ppm): δ 8.55 (s, Pery), 6.90-6.49 (s, C*H*=C*H* on backbone), 4.76-4.21 (d, OCH_2CH_2N), 4.20-3.87 (s, NCH_2CH), 3.27-2.76 (t, CH_2C*H*CH_2 on rings), 2.09-1.12 (m, hydrogen on alkyl chain), 0.89 (s, CH_3).

Monomer **3** (200 mg, 0.143 mmol) and **Ru-III** (5.0 mg, 5.7 μmol) were stirred in 24 mL of $CHCl_3$ at 50 °C for 1 h. ^1H NMR (500 MHz, $CDCl_3$, ppm): δ 8.67 (s, Pery), 7.29-6.87 (m, C*H*=C*H* on phenyl), 5.92-5.64 (s, *trans*-C*H* on backbone), 5.63-5.32 (s, *cis*-C*H* on backbone), 4.43-4.03 (d, NCH_2), 3.33-3.00 (d, COC*H*CH), 2.98-2.71 (m, CHCH_2). 2.68-2.17(CH_2COO+CHC*H*CH),1.97-0.99 (m,NCH_2(CH_2)$_9$$CH_2$COO); ^{13}C NMR (125 MHz, $CDCl_3$, ppm): δ 176.72, 171.62, 162.18, 150.14, 135.28, 132.90, 131.45, 129.21, 128.49, 127.55, 127.26, 123.21, 122.05, 51.11, 46.01, 40.91, 30.94, 29.09, 27.95, 26.82, 24.72.

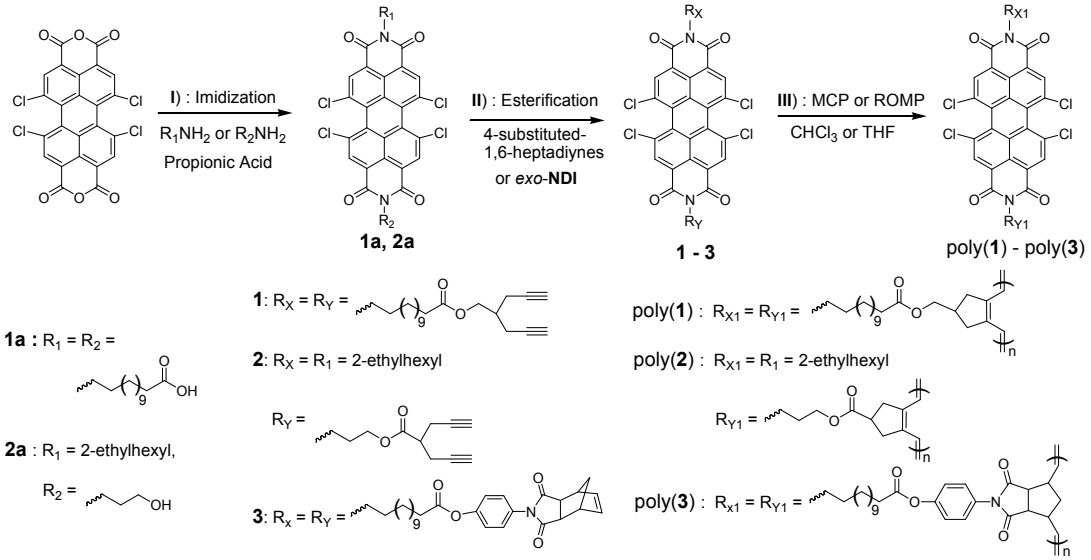

Scheme S1. The synthetic routes for **1 - 3** and the relative polymers: I) Imidiation of PBI with the corresponding amines to obtain **1a** and **2a**; II) Esterification reaction of **1a** and **2a** to obtain **1 - 3**, 4-substituted-1,6-heptadiynes are 4-hydroxymethyl-1,6-heptadiyne and 2-(2-propinyl)-4-pentinoic acid, and *exo*-**NDI** is exo-N-(4-hydroxy phenyl)-norbornenepyrrolidine; III) MCP and ROMP of **1 - 3** to obtain relative polymers.

With the obtained monomers **1**, **2**, and **3** in hand (Scheme S1 in the ESI), the relative polymers were subsequently synthesized by MCP or ROMP, and the results are collected in Table S1. It should be noted that solubility plays an important role in solution characterization of polymer and solution-processed organic electronic devices. As the poor solubility of PBI segments and the conjugated PA backbone is concerned, MCP of monomer bearing long alkyl chain between bis(1,6-heptadiyne) groups and PBI core was explored to ensure the solubility of polymer. When **Ru-III** was added to the solution of **1**, the orange color immediately changed to yellow-green, then turned gradually to dark-red, and finally the dark-red double-stranded PA, poly(**1**), was obtained by precipitating the mixture from excess acetone in various yields. With a lower molar feed ratio of **1** to **Ru-III** ([M]/[I]) of 25, 85 % of **1** was

converted into poly(**1**) with relatively low degree of polymerization (DP = 19) and narrow molecular weight distribution (PDI = 1.4) in $CHCl_3$ at 50 °C (Run 1). As expected, poly(**1**) can be easily soluble in common organic solvents such as CH_2Cl_2 and THF, while insoluble in N,N'-dimethylformamide (DMF) (Table S2). With increasing monomer loading, the higher [M]/[I] ratios of 50 and 100 (Runs 2 and 3) were attempted for expecting to obtain higher molecular weight polymers, whereas the maximum DP was only up to 25 in these cases, even prolonged reaction time to 24 h (Run 4), and the isolated yields sharply reduced to 36 % and 22 % accordingly. All results suggested that the propagating carbenes vanished in $CHCl_3$ when the conjugated polymer chain length increased to a certain size, likely due to the propagating carbenes decomposed during the MCP process in noncoordinating solvent.[4]

Table S1 Characteristics for polymerization and the resultant polymers

Run	Polymer	[M]/[I][a]	M_n[b] (kDa)	PDI[b]	DP[c]	Yield (%)
1	poly(**1**)	25:1	21.6	1.4	19	85
2	poly(**1**)	50:1	27.7	1.4	24	36
3	poly(**1**)	100:1	28.2	1.4	25	22
4	poly(**1**)[d]	100:1	28.4	1.4	25	26
5	poly(**1**)[e]	50:1	41.7	1.2	37	96
6	poly(**1**)[e]	100:1	81.1	1.2	72	72
7	poly(**2**)	25:1	16.6	1.4	20	99
8	poly(**2**)	50:1	18.8	1.3	23	86
9	poly(**2**)	100:1	20.1	1.4	25	85
10	poly(**2**)[e]	100:1	100.4	1.3	130	99
11	poly(**3**)	25:1	27.3	1.5	23	95

Polymerization conditions: using **Ru-III** as catalyst, $CHCl_3$ or THF as solvent, 50 °C, 3 h, [M] = 1 ~ 8×10^{-3} mol/L for double-stranded polymers, and 0.5 mol/L for single-stranded polymers.

[a] The molar ratio of monomer to initiator.

[b] Determined by GPC in THF relative to monodispersed polystyrene standards.

[c] Degree of polymerization.

[d] Polymerization conditions: 50 °C, 24 h, [M] = 8×10^{-3} mol/L in $CHCl_3$.

[e] Polymerized in THF and the GPC data was tested in 1,2,3- trichlorobenzene relative to monodispersed polystyrene standards.

Similar results were found for the synthesis of single-stranded poly(**2**) in $CHCl_3$, when the molar ratio of [M]/[I] was 25 (Run 7), the resultant polymer has the DP of 20 in 99 % yield. Increased [M]/[I] ratios from 50 to 100 were then adopted (Runs 8 and 9), the corresponding polymers have slightly higher DPs of 23 and 25 in decreased yields of 86 % and 85 %, respectively, and they were soluble in most of organic solvents. ROMP of **3** was also conducted in $CHCl_3$ accompanying with the

color change from orange to red-orange when **Ru-III** was added to the solution of **3** for a while, generating the resultant double-stranded poly(norbornene-dicarboximide) derivative, poly(**3**) (Run 11), which is completely soluble in $CHCl_3$, CH_2Cl_2, and DMF, but little soluble in THF, this may be related to the more polar imide moiety and non-conjugated backbone.

For comparing polymerization behavior and enhancing the monomer conversion, a simple and efficient strategy is to change the solvent.[4] MCP of **1** was then carried out with higher [M]/[I] ratios of 50 and 100 in THF (Runs 5 and 6), a weakly coordinating solvent, produced the polymers with DP of 37 in 96 % yield under the former condition, while in the latter case the polymer precipitated out from THF solvent in decreased yield of 72 % as well as a high DP of 72. The precipitated poly(**1**) could be dissolved in $CHCl_3$, CH_2Cl_2, and chlorobenzene. Based on this result, a primary conclusion can be drawn that poly(**1**) with higher molecular weight has worse solubility in THF. Similarly, the cyclopolymerization of **2** with high [M]/[I] ratio of 100 in THF proceeded smoothly, and the obtained poly(**2**) has much higher DP of 130 in 99 % yield (Run 10). Apparently, the values of yield and DP for poly(**1**) and poly(**2**) in THF are much higher than those in $CHCl_3$ under the same conditions, suggesting that THF coordination can be an effective means of stabilizing propagating carbenes. As proved by Choi[4] that using a weakly coordinating solvent greatly improved the catalyst lifetime by stabilizing the propagating species through solvent coordination. Contrarily, the propagating carbenes vanished during the MCP process in $CHCl_3$, implying rapid decomposition of the active carbenes in noncoordinating solvents. This vast difference in the stability of the propagating species containing the long conjugated carbene may be the key factor that allowed great enhancement of the conversion when the MCP was performed in THF.

Table S2 Solubility of polymers in various solvents at room temperature*

	xylene	THF	CH_2Cl_2	DCB	DMF	1,4-dioxane
poly(**1**)	+	+	+	+	–	+
poly(**2**)	+	+	+	+	–	+
poly(**3**)	+	+–	+	+	+	+

*1 mg of polymer in 1 mL of solvent;

– : insoluble; +– : partially soluble; + : soluble; DCB: o-dichlorobenzene.

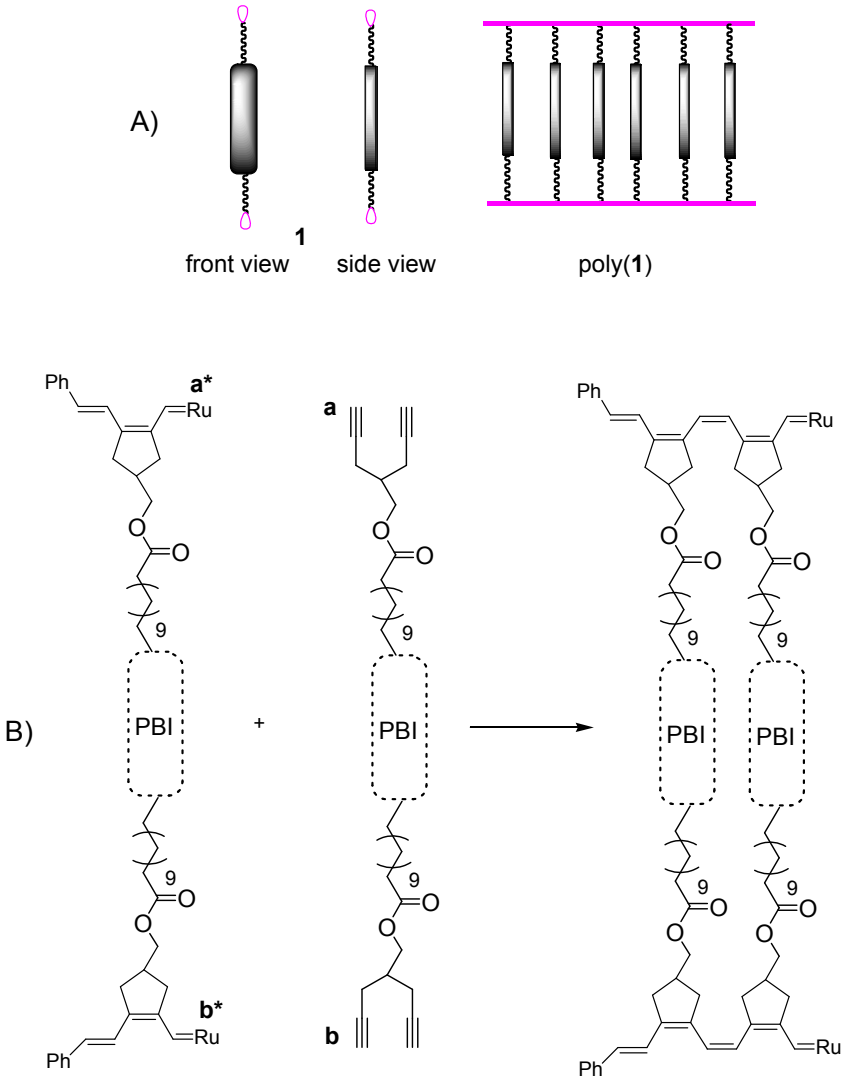

Scheme S2. Schematic illustration of **1** and poly(**1**) by cartoon picture (A) and polymerization process of **1** toward ladder-like poly(**1**) (B).

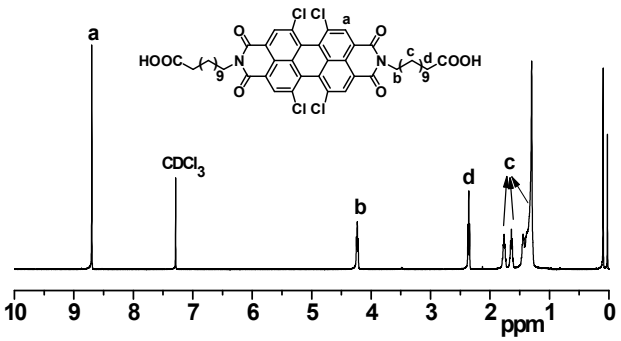

Figure S1. ^{1}H NMR spectrum of **1a**.

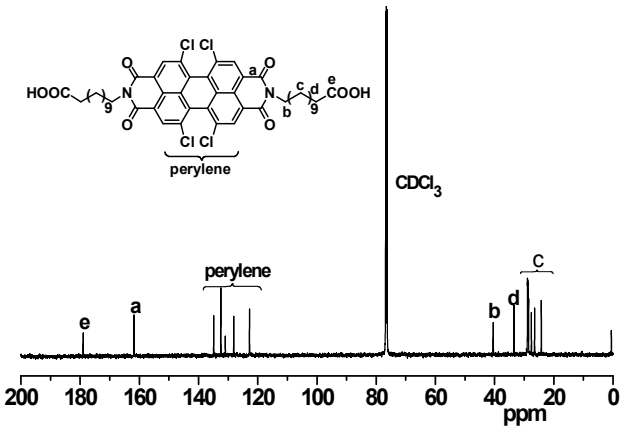

Figure S2. ^{13}C NMR spectrum of **1a**.

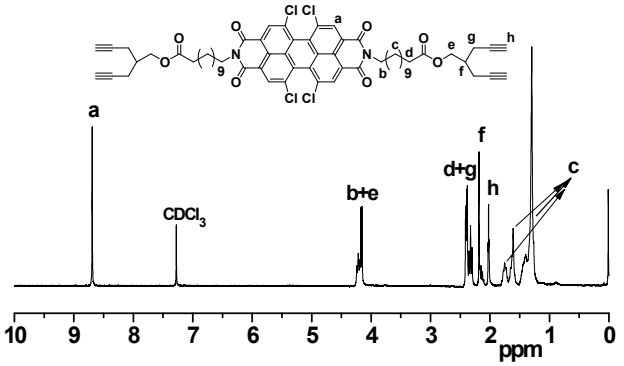

Figure S3. ^{1}H NMR spectrum of **1**.

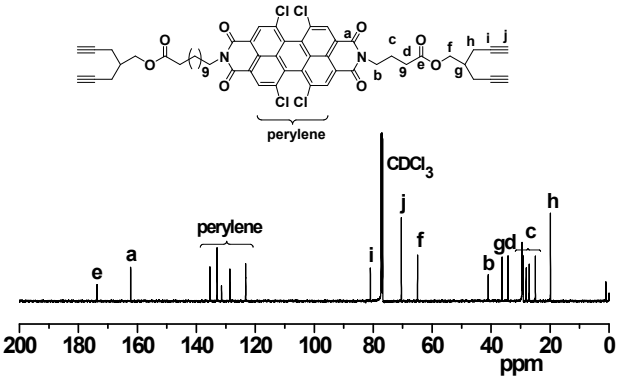

Figure S4. ^{13}C NMR spectrum of **1**.

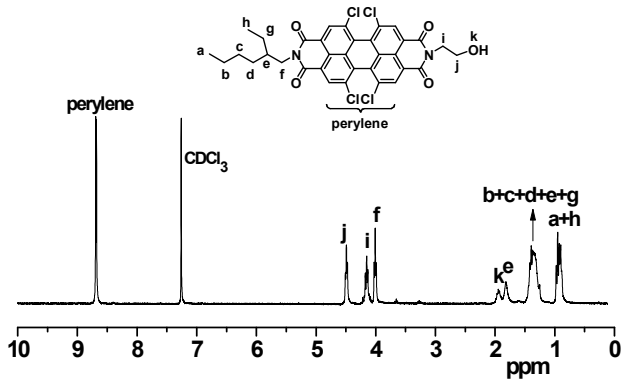

Figure S5. ^{1}H NMR spectrum of **2a**.

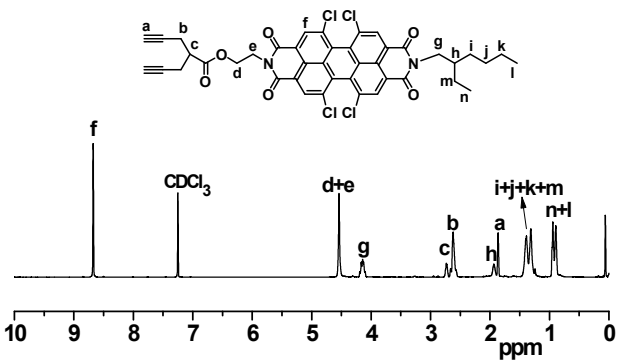

Figure S6. [1]H NMR spectrum of **2**.

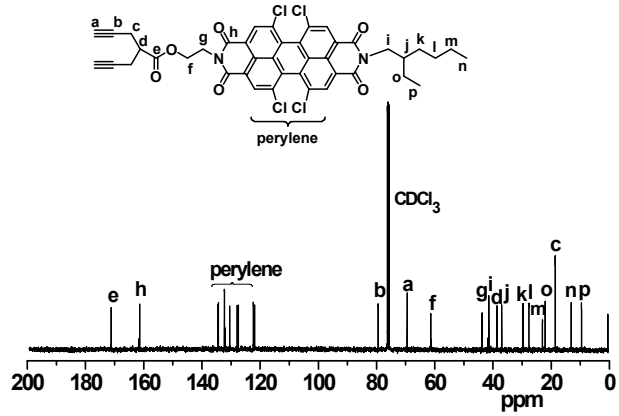

Figure S7. [13]C NMR spectrum of **2**.

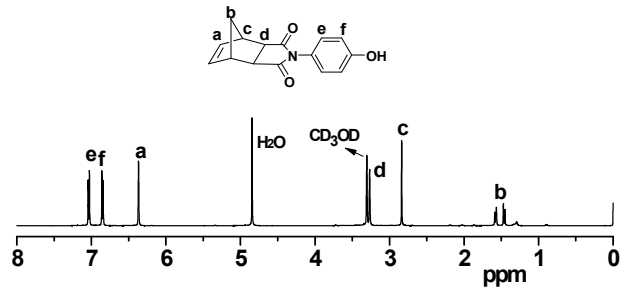

Figure S8. [1]H NMR spectrum of *exo*-**NDI**.

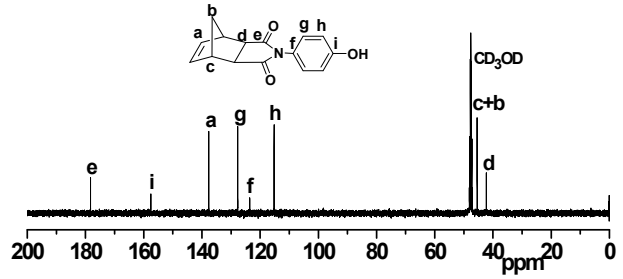

Figure S9. [13]C NMR spectrum of *exo*-**NDI**.

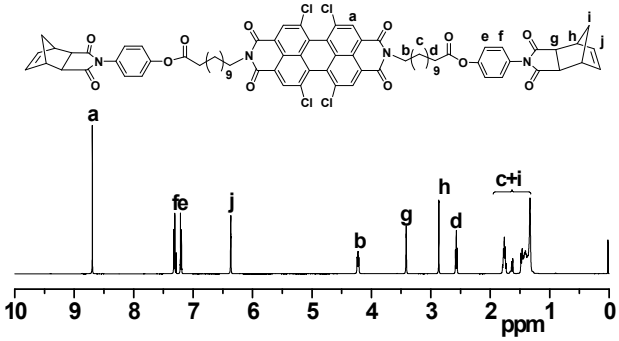

Figure S10. ^{1}H NMR spectrum of **3**.

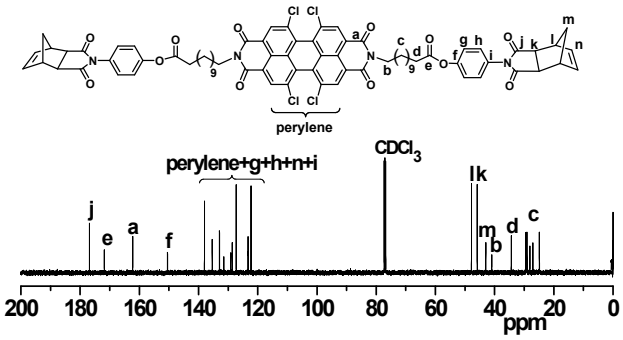

Figure S11. ^{13}C NMR spectrum of **3**.

As the polymerization proceeded, the peak of acetylenic proton (H_h, Fig. S3) for **1** at 2.02 ppm disappeared, and a symmetric broad peak was observed at 6.53 ppm for the polyene protons (H_h, Fig. S12) on the conjugated backbone of poly(**1**). It is noteworthy that the presence of this single broad peak may imply that the double bonds of poly(**1**) should have the same (*cis*) configuration. The peaks of acetylenic carbons (C_{j+i}, Fig. S4) for the 1,6-heptadiyne moiety, which should appear between 70 and 81 ppm, were not seen in the ^{13}C NMR spectrum of poly(**1**). Instead, the peak of the methylene carbon (C_f) on CH_2O group appears at 67.1 ppm (Fig. S13). On the basis of the symmetrical single peak at 6.53 ppm and the single peak at 67.1 ppm, it is suggested that MCP triggered by initiator **Ru-III** produced poly(**1**) with exclusively five-membered ring units, i.e., 1,2-(cyclopent-1-enylene)-vinylenes.

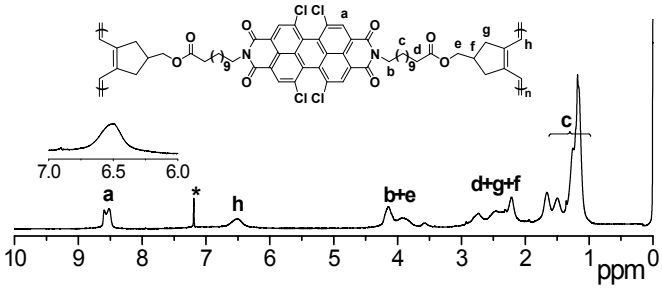

Figure S12. ^{1}H NMR spectrum of poly(**1**)..

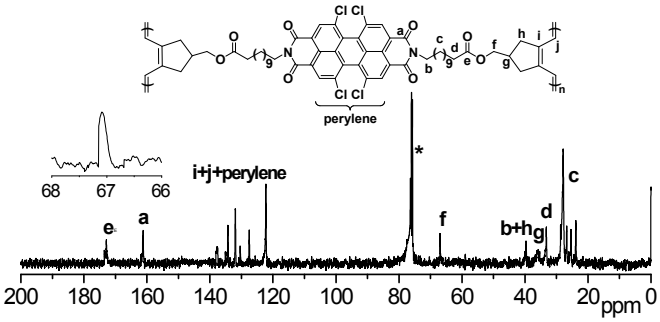

Figure S13. ^{13}C NMR spectrum of poly(**1**) (*denotes solvent).

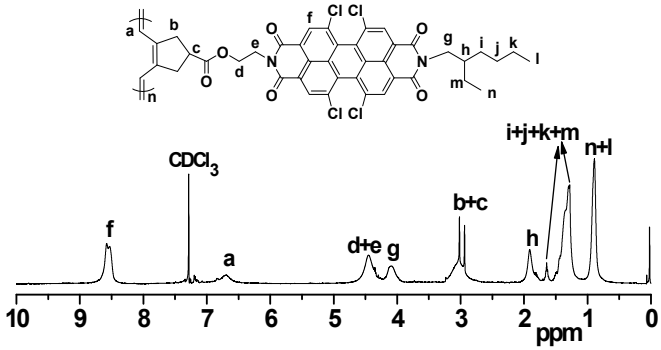

Figure S14. ^{1}H NMR spectrum of poly(**2**).

For poly(**3**), the signal of olefinic protons on the norbornene ring at 6.36 ppm (H_j, Fig. S10) completely disappeared after ROMP, while two new signals of olefinic protons (H_i) on the backbone came at 5.79 and 5.52 ppm (Fig. S15), indicating that poly(**3**) has both *trans* and *cis* double bonds, and the *trans*/*cis* ratio is nearly 1 : 1 based on the calculation of peak areas from the corresponding ^{1}H NMR spectrum.

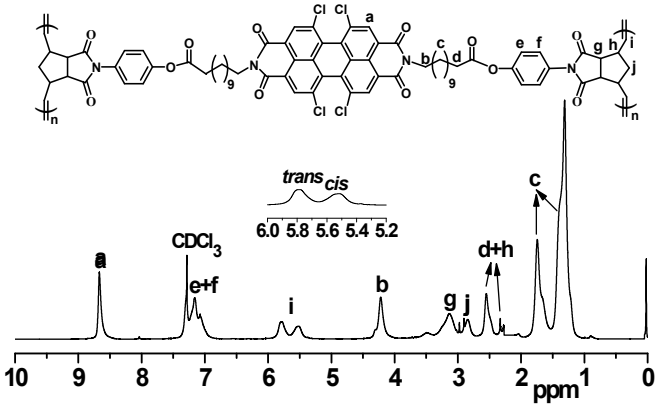

Figure S15. ^{1}H NMR spectrum of poly(**3**).

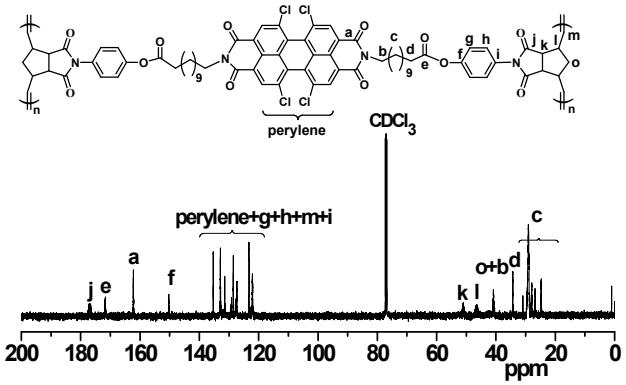

Figure S16. ^{13}C NMR spectrum of poly(**3**).

The infrared spectrum of poly(**1**) (Fig. S17) shows neither the acetylenic hydrogen stretching nor the carbon-carbon triple-bond stretching which are expected to be present at 3320 and 2120 cm^{-1} for **1**, respectively. While the shoulder peak at 2850 cm^{-1} and the peak at 750 cm^{-1} were assigned to the unsaturated =C-H and C-Cl stretching vibrations, respectively. The vibration of the external plane of C-H on aromatic ring at 900 cm^{-1} and the bending vibration at 800 cm^{-1} were also observed. For **2** and poly(**2**), similar results were observed by IR spectra (Fig. S18).

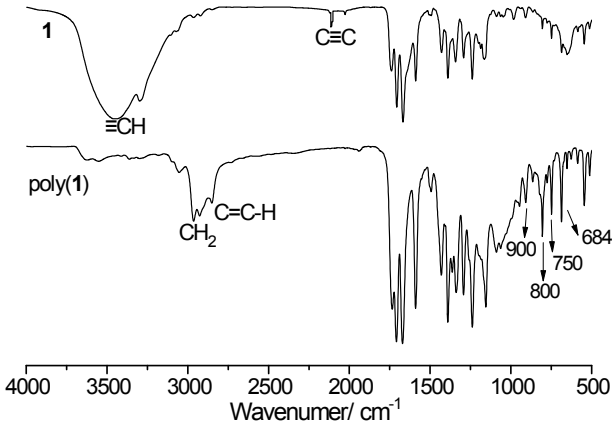

Figure S17. IR spectra of **1** and poly(**1**).

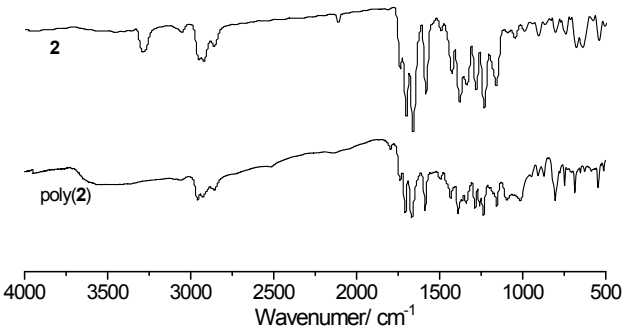

Figure S18. IR spectra of **2** and poly(**2**).

The typical fluorescence changes are shown in Figure S19, which is indicative of

the transformation from monomer to polymer. The dilute $CHCl_3$ solutions of **1** - **3** are highly emissive under UV illumination at 365 nm and 254 nm (Figure S19a) or excited at 520 nm (Figure S19b); after polymerization, the fluorescence of poly(**1**) is quenched. This behavior is in good consistent with the previous reported results,[5] because the conjugated PA backbone possibly works as a quenching site for light emission, which absorbs the light emitted from the PBIs. Also, the fluorescence of poly(**2**) shared the same result of poly(**1**). Contrarily, the $CHCl_3$ solution of non-conjugated poly(**3**) showed yellow fluorescence as that of **3** though the intensity decreased, which is much different from the conjugated poly(**1**) and poly(**2**).

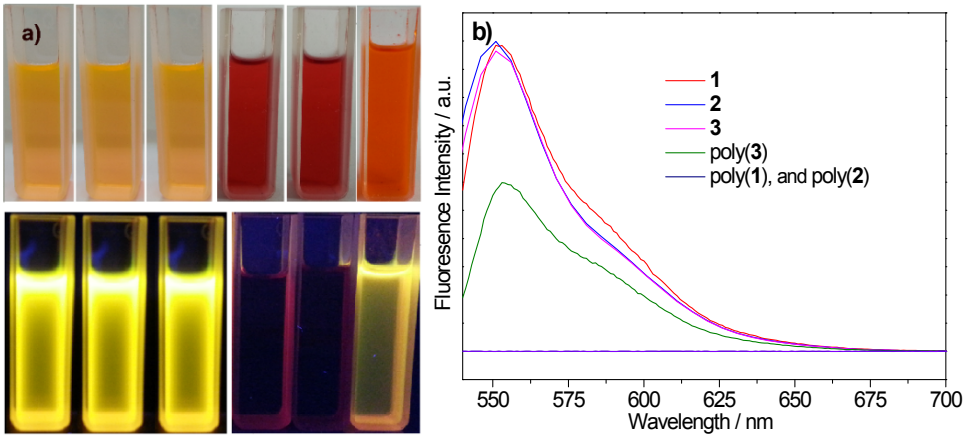

Figure S19. a) Photographs of monomers (**1** - **3**) and the relative polymers (poly(**1**), poly(**2**), and poly(**3**) from left to right) in $CHCl_3$ solution upon 365 nm (top) and 254 nm (bottom) illumination; b) fluorescence spectra of monomers and polymers measured in $CHCl_3$ excited at 520 nm.

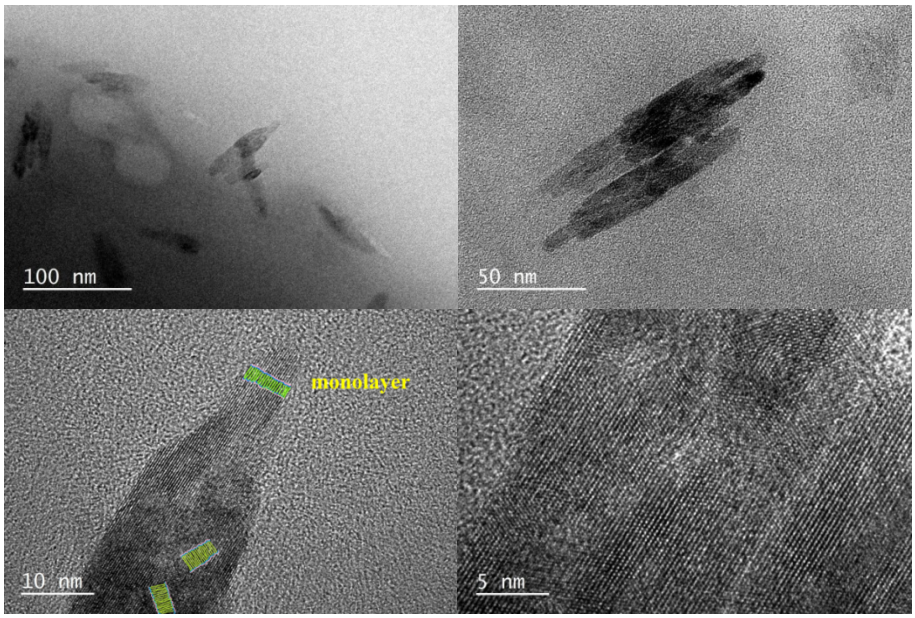

Figure S20. HR-TEM images of poly(**1**).

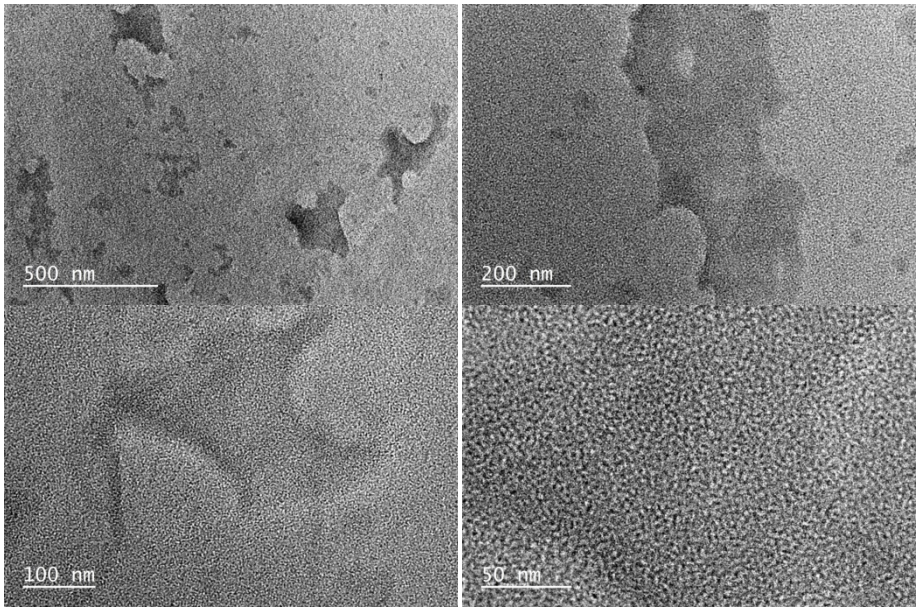

Figure S21. TEM images of poly(**2**).

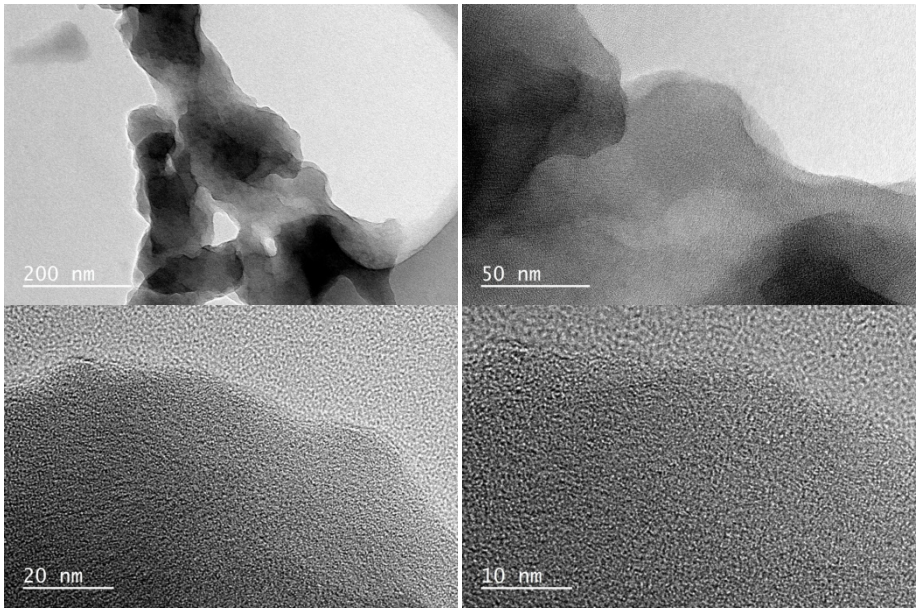

Figure S22. TEM images of poly(**3**).

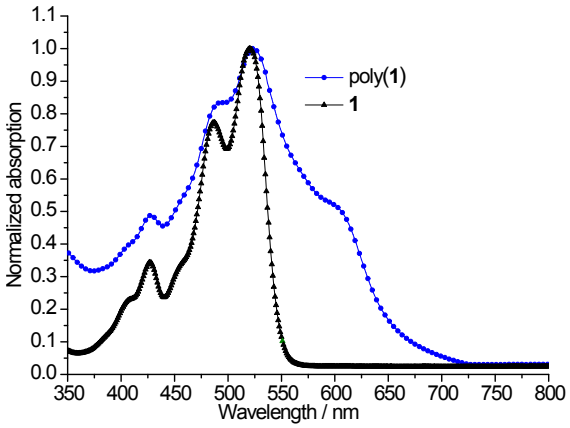

Figure S23. UV-vis spectra of **1** and poly(**1**) in $CHCl_3$.

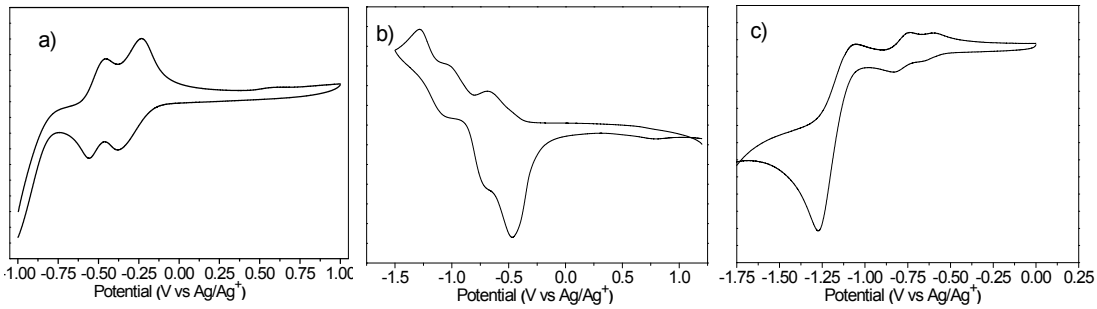

Figure S 24. CV curves of a) poly(**1**), b) poly(**2**), and c) poly(**3**).

The CV results implied that we can tune the energy difference ($LUMO_{(A)}$ − $HOMO_{(D)}$) between the LUMO of acceptor (A) and the HOMO of donor (D) by regulating the LUMO energy of PBI-based polymers (Fig. S25).[6] As to the stability of organic compounds and polymers, it is believed that the HOMO of *p*-type organic semiconductors (such as P3HT) should be more negative than -5.0 eV, e.g., locating at -5.0 to -6.0 eV, and the LUMO of *n*-type organic semiconductors is best located between -4.0 and -4.5 eV, for anti-oxidation in air. Therefore, poly(**1**) matched quite well with the requirement. It seems that the PBI-based **PA**s by MCP own greater prospects than PBI-LPS[7] and P1-endo(P2-exo),[8] not only from the utilization of sunlight but also from the ambient stability of polymers.

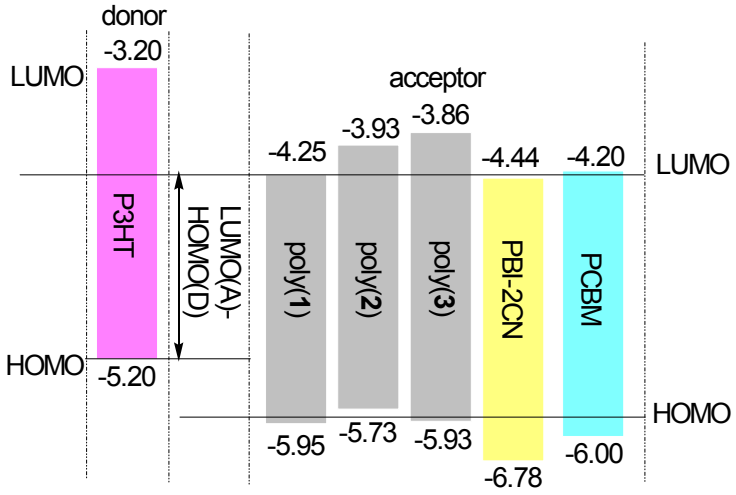

Figure S 25. Energy level diagrams of a donor and various acceptors.

Although the oxidative stability of poly(1,6-heptadiyne) derivatives reported previously had been enhanced over those unsubstituted analogous poly(1,6-heptadiyne), decomposition of a long, π-conjugated polyene framework could not be avoided completely.[9] The oxidative stability of polymers was tracked by UV−vis spectroscopy (Figure S26). The conjugated poly(**DDDPM**) with two long alkyl side groups was extremely unstable in THF (Figure S26a), as time proceeded, the original

rose-carmine solution gradually faded until colorless within 3 days. Correspondingly, the λ_{max} gradually blue shifted from 550 nm to 500 nm after standing for 2 days, and the absorption overall intensity decreased, which is reflected by the reduced M_n of polymer from 15.2 to 4.2 kDa (Figure S27), indicating the conjugated length shortened. Poly(1,6-heptadiyne) even with a bulky substituent such as triphenylamine was also unstable in THF (Figure S26b), though it decomposed slightly slower than poly(**DDDPM**). Astonishingly, there is no obvious change occurred in the UV-vis spectra of poly(**1**) (Figure S26c) and poly(**2**) (Figure S26d), they were extremely stable in THF even prolonged time to 30 days. The stability of them was originated from the effective shielding of oxygen by the steric bulky PBI substituents,[10] which is particularly important in synthetic stable polyene chemistry, especially in the solar cell application.

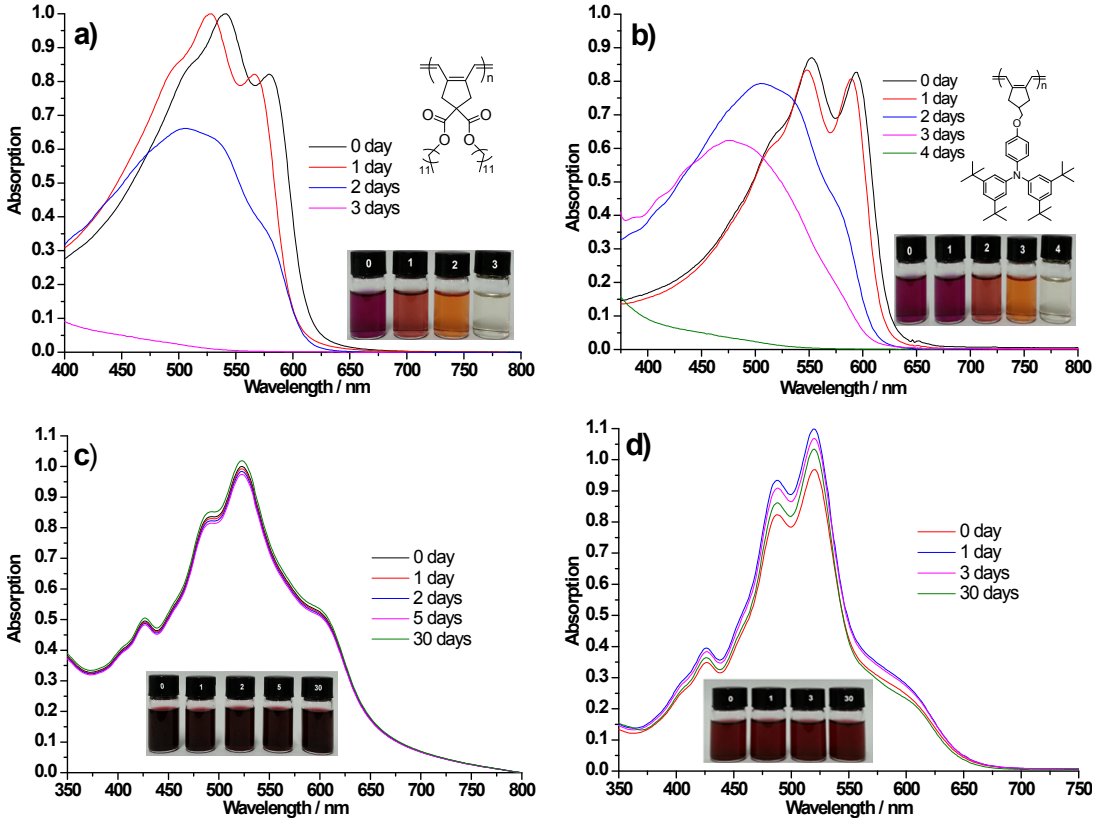

Figure S26. UV-vis spectra and relative pictures of conjugated polymers in THF solution: a) poly(**DDDPM**), b) PA with triphenylamine pendant, c) poly(**1**), and d) poly(**2**).

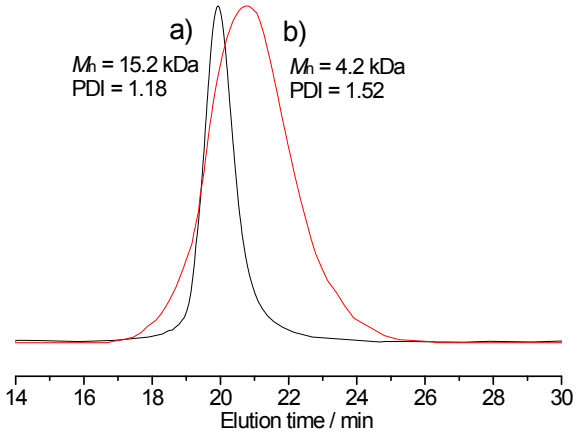

Figure S27. GPC traces of poly(**DDDPM**) a) before and b) after oxidative degradation.

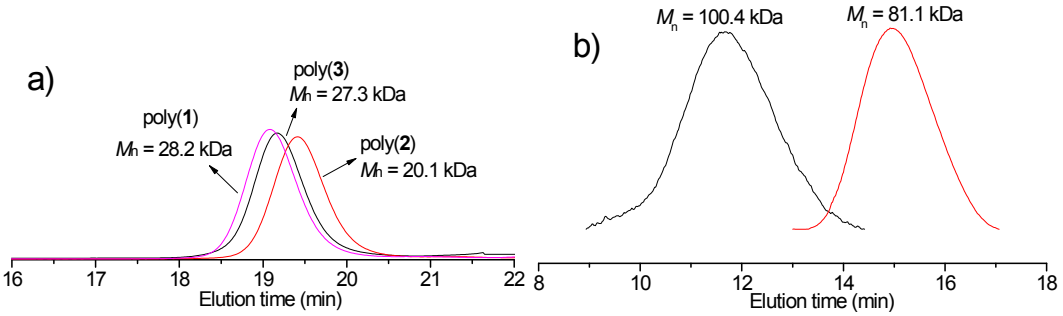

Figure S28. Representative GPC traces of polymers measured a) in THF and b) in 1,2,3-trichlorobenzene.

The thermal stability of polymers was investigated by means of thermal gravimetric analysis. As shown in Fig. S29, double-stranded poly(**1**) began to decompose at 308 °C, and 5 wt. % loss temperature (T_d) is reached to 367 °C, even when the polymer was heated to 800 °C, 54 % of weight was still retained, indicating the excellent thermal stability of poly(**1**). Double-stranded poly(**3**) was similar to that of poly(**1**). While single-stranded poly(**2**) began to decompose at 197 °C, T_d is only 254 °C, and it retains 26 % of weight at 800 °C. The results fully confirmed the better thermal resistance of double-stranded polymers, which is also important for the practical application of polymers in devices and circuits, especially when they are used under high temperature.

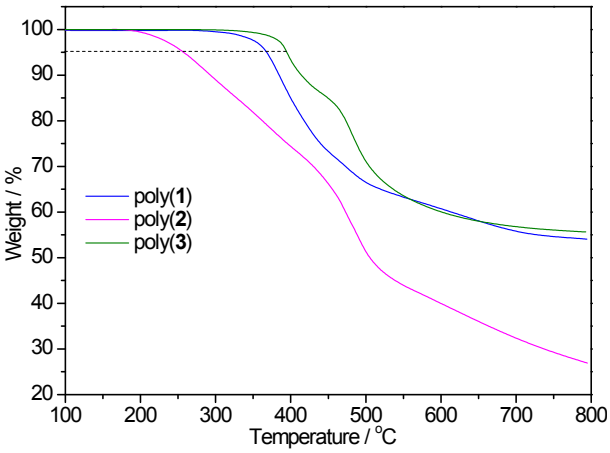

Figure S29. TGA curves of polymers.

References

1. J. M. Carney, P. J. Donoghue, W. M. Wuest, O. Wiest and P. Helquist, *Org. Lett.*, 2008, **10**, 3903.
2. J. A. Love, J. P. Morgan, T. M. Trnka and R. H. Grubbs, *Angew.Chem. Int. Ed.*, 2002, **41**, 4035.
3. F. J. Céspedes-Guirao, K. Ohkubo, S. Fukuzumi, A. Sastre-Santos and F. Fernández-Lázaro, *J. Org. Chem*., 2009, **74**, 5871.
4. E.-H. Kang, I. S.Lee and T.-L. Choi, *J. Am. Chem. Soc.*, 2011, **133**, 11904.
5. J. Qu, Y. Suzuki, M. Shiotsuki, F. Sanda and T. Masuda, *Polymer*, 2007, **48**, 4628.
6. E. Zhou, J. Cong, Q. Wei, K. Tajima, C. Yang and K. Hashimoto, *Angew. Chem. Int. Ed.*, 2011, **50**, 2799.
7. W. Fu, C. He, S. Jiang, Z. Chen, J. Zhang,; Z. Li, S. Yan and R. Zhang, *Macromolecules*, 2011, **44**, 203.
8. W. Fu, C. He and Z. Li, *J. Polym. Sci., Part A: Polym. Chem.*, 2012, **50**, 1333.
9. S.-K. Choi, Y.-S. Gal, S.-H. Jin and H. K. Kim, *Chem. Rev.*, 2000, **100**, 1645.
10. S.-H. Kim, Y.-H. Kim, H.-N. Cho, S.-K. Kwon, H.-K. Kim and S.-K. Choi, *Macromolecules*, 1996, **29**, 5422.